HHS Public Access

Author manuscript

Neuroscience. Author manuscript; available in PMC 2019 November 01.

Published in final edited form as:

Neuroscience. 2018 November 01; 391: 91–103. doi:10.1016/j.neuroscience.2018.09.008.

Glutamatergic Projections to the Cochlear Nucleus are Redistributed in Tinnitus

Amarins N. Heeringa[a], **Calvin Wu**[a], **Christopher Chung**[a], **Michael West**[a], **David Martel**[a], **Leslie Liberman**[b], **M. Charles Liberman**[b], and **Susan E. Shore**[a]

[a]Kresge Hearing Research Institute; Otolaryngology, University of Michigan, Ann Arbor, MI 48104, USA

[b]Eaton-Peabody Laboratories, Massachusetts Eye and Ear Infirmary, and Department of Otolaryngology, Harvard Medical School, Boston, MA 02114, USA

Abstract

Tinnitus alters auditory-somatosensory plasticity in the cochlear nucleus (CN). Correspondingly, bimodal auditory-somatosensory stimulation treatment attenuates tinnitus, both in animals and humans (Marks et al., 2018). Therefore, we hypothesized that tinnitus is associated with altered somatosensory innervation of the CN. Here, we studied the expression of vesicular glutamate transporters 1 and 2 (VGLUT1 and VGLUT2) in the CN, which reveals glutamatergic projections from the cochlea as well as somatosensory systems to this brainstem auditory center.

Guinea pigs were unilaterally exposed to narrowband noise and behaviorally tested for tinnitus using gap-prepulse inhibition of the acoustic startle. Following physiological and behavioral measures, brain sections were immunohistochemically stained for VGLUT1 or VGLUT2. Puncta density was determined for each region of the ipsilateral and contralateral CN.

Tinnitus was associated with an ipsilateral upregulation of VGLUT2 puncta density in the granule cell domain (GCD) and anteroventral CN (AVCN). Furthermore, there was a tinnitus-associated interaural asymmetry for VGLUT1 expression in the AVCN and deep layer of the dorsal CN (DCN3), due to contralateral downregulation of VGLUT1 expression. These tinnitus-related glutamatergic imbalances were reversed upon bimodal-stimulation treatment.

Tinnitus-associated ipsilateral upregulation of VGLUT2-positive projections likely derives from somatosensory projections to the GCD and AVCN. This upregulation may underlie the neurophysiological hallmarks of tinnitus in the CN. Reversing the increased ipsilateral glutamatergic innervation in the CN is likely a key mechanism in treating tinnitus.

Corresponding author: Susan Shore, Kresge Hearing Research Inst. 1100 W. Medical Center Drive, Ann Arbor, MI 48104, USA. Tel: 734-647-2116; Fax: 734-764-0014; sushore@umich.edu.

SES Designed research; ANH, CC, MW, DM, and LL Performed research; ANH, CW, CC, and DM Analyzed data; ANH, SES, CW, and MCL Wrote the paper.

Dr. M. C. Liberman has an equity interest in Decibel Therapeutics. The other authors declare no competing financial interests.

Keywords

Auditory; Cross-modal compensation; Noise exposure; Synaptopathy; VGLUT1; VGLUT2

Introduction

Tinnitus, or ringing in the ears, is defined as an auditory sensation in the absence of a corresponding external sound source and affects approximately 10–15 % of the world's population (Bhatt et al., 2016; Shore et al., 2016). Tinnitus appears to be correlated with aberrant neural activity along the central auditory pathway, including in the cochlear nucleus (CN) (Eggermont and Roberts, 2015; Shore et al., 2016). In animal models of tinnitus, fusiform cells, the principal output neurons of the dorsal CN (DCN), show increased spontaneous firing rates, enhanced synchrony, and enhanced bursting (Brozoski et al., 2002; Kaltenbach et al., 2004; Dehmel et al., 2012; Wu et al., 2016a).

In addition to processing auditory information from the auditory nerve, the CN also receives input from other sensory modalities including brainstem nuclei of the somatosensory system, the spinal trigeminal nucleus (Sp5) and the cuneate nucleus (Zhou and Shore, 2004; Haenggeli et al., 2005; Zeng et al., 2011). Previous studies have shown that auditory-somatosensory plasticity in the DCN is altered following tinnitus (Dehmel et al., 2012; Koehler and Shore, 2013; Marks et al., 2018). This neural correlate of tinnitus is likely to be associated with "somatic tinnitus", in which tinnitus sufferers can modulate the loudness and pitch of their tinnitus by somatic maneuvers such as jaw clenching (Levine, 1999; Sanchez et al., 2002; Ostermann et al., 2016).

Projections from the somatosensory system to the CN terminate primarily in the granule cell domain (GCD), which encompasses regions that contain granule and small cells that surround the ventral CN (VCN) and form a layer between the molecular and deep layers of the DCN. Somatosensory projections terminate to a lesser extent in the magnocellular regions of the anteroventral CN (AVCN) and posteroventral CN (PVCN) and in the deep layer of the DCN (DCN3) (Zhou and Shore, 2004; Haenggeli et al., 2005; Zeng et al., 2011). The somatosensory-to-CN projection is glutamatergic (Haenggeli et al., 2005; Zhou et al., 2007; Zeng et al., 2012) and can be distinguished from auditory nerve glutamatergic projections by the subtype of the vesicular glutamate transporter (VGLUT), which mediates pre-synaptic uptake of glutamate into synaptic vesicles (Takamori et al., 2000, 2001; Fremeau et al., 2002). Type I auditory nerve fibers, the myelinated component of the primary sensory nerve, co-label exclusively with the subtype VGLUT1, whereas somatosensory projections primarily co-label with the subtype VGLUT2 and to a minor extent with VGLUT1 in normal-hearing animals (Zhou et al., 2007; Zeng et al., 2012). Thus, studying the distributions of glutamatergic markers, VGLUT1 and VGLUT2, across regions of the CN provides insight into the relative innervation of the CN by the auditory nerve and other, non-cochlear systems, including the somatosensory system.

Previous studies have shown that severe cochlear damage results in a redistribution of VGLUT subtypes in the CN: auditory nerve-associated VGLUT1 expression decreases and non-auditory nerve-associated VGLUT2 expression increases (Zeng et al., 2009; Barker et

al., 2012; Heeringa et al., 2016). In particular, the increases in VGLUT2 expression following unilateral cochlear damage corresponds to an upregulation of somatosensory projections to the CN (Zeng et al., 2012). We hypothesized that similar cross-modal compensation in the CN contributes to altered auditory-somatosensory plasticity in tinnitus. Here, we studied VGLUT1 and VGLUT2 expression across CN regions in unilaterally noise-exposed animals with and without behavioral evidence of tinnitus. Tinnitus animals showed an ipsilateral upregulation of VGLUT2 puncta, possibly derived from somatosensory projections to the CN, which was reversed following bimodal auditory-somatosensory stimulation treatment that can reverse tinnitus in animals and humans (Marks et al., 2018).

Experimental Procedures

Experimental set-up

Twenty-four adult pigmented guinea pigs of either sex (Elm Hill Laboratories, 2–3 weeks of age) were used in this study. Animals were socially housed and had *ad libitum* access to food and water. Animals were unilaterally noise- or sham-exposed twice, with a period of four weeks between exposures. To determine the presence of tinnitus, gap pre-pulse inhibition of the acoustic startle reflex (GPIAS) was assessed before and after noise exposures (Turner et al., 2006; Berger et al., 2013; Wu et al., 2016a). Following tinnitus assessment, a subset of tinnitus animals was treated with a custom-designed bimodal-stimulation treatment to reverse tinnitus (Marks et al., 2018). For final data analysis, animals were divided into 4 groups: 6 sham-exposed control animals (N), 8 noise-exposed no-tinnitus animals (ENT), and 10 noise-exposed tinnitus animals (ET), of which 4 were treated with the bimodal-stimulation paradigm (ET_T). *In vivo* neurophysiological recordings of DCN fusiform cells were performed 12 weeks following the last exposure after which the animals were transcardially perfused and cochleae and brains were collected for further processing. Neurophysiological results are described in previous reports (Wu et al., 2016a; Marks et al., 2018). All procedures were approved by the University's laboratory animal care and use committee, conformed to the NIH Guide for the Care and Use of Laboratory Animals, and followed the Society for Neuroscience's Guidelines for the Use of Animals in Neuroscience Research.

Noise exposure

Animals were anesthetized with ketamine (40 mg/kg, Putney) and xylazine (10 mg/kg, Lloyd) and were unilaterally exposed to the left ear with narrow-band noise (centered at 7 kHz, 0.4 octave bandwidth, 97 dB SPL for 2h). The exposure was repeated after four weeks. Sham-exposed animals underwent the same procedures, without turning on the intense noise.

Auditory brainstem responses

Cochlear thresholds were determined by auditory brainstem responses (ABR) recorded before (t0), immediately after (t1), and pre-surgery (tf; see Figure 3A) (Wu et al., 2016a). ABR stimuli (8 kHz, 12 kHz, and 16 kHz tone bursts, 0–90 dB SPL in 10 dB steps, 2 ms cos^2 rise/fall times, 1024 repetitions, 30 Hz presentation rate) were presented using

SigGenRP and BioSigRP (Tucker-Davis Technologies Inc. [TDT]). Subdermal electrodes were placed on the vertex and behind each pinna for reference, recording, and grounding, respectively. ABR waveforms were visually inspected for threshold, defined by the lowest stimulus level in which wave 4 (the largest wave) was clearly detectable. Wave 1 amplitude, representing auditory nerve firing (P1-N1), was determined for each stimulus level and frequency using a custom MatLab program.

Tinnitus assessment

The presence of tinnitus was determined using GPIAS as previously described (Turner et al., 2006; Koehler and Shore, 2013; Wu et al., 2016a; Marks et al., 2018). Briefly, the animal's startle reflex in response to a 20 ms, 95 dB SPL broadband noise pulse was measured by video tracking the pinna Preyer's reflex (Berger et al., 2013; Wu et al., 2016a). A 50 ms silent gap in a 65 dB SPL constant background carrier (band limited at 8–10, 12–14, or 16–18 kHz) was presented 100 ms before the startle pulse. In normal-hearing, unexposed animals, this inhibits the Preyer's startle reflex (Berger et al., 2013). GPIAS was assessed before and after noise or sham exposures over a period of 4 weeks and following bimodal-stimulation treatment. An animal was defined as having tinnitus if its post-exposure gap startle suppression distribution was significantly greater (established by a one-tailed T-test at 0.05 alpha) than the baseline gap startle suppression distribution in the same animal for any carrier frequency. To control for hearing loss and temporal processing anomalies due to the noise exposure, the silent gap-in-noise was replaced by a narrowband, noise pre-pulse (75 dB SPL). The pre-pulse had the same characteristics as the constant background carrier in which the silent gap was embedded.

Bimodal-stimulation treatment

Four tinnitus animals (ET_T) were treated with a bimodal auditory-somatosensory stimulation treatment designed to reduce tinnitus, based on stimulus-timing dependent plasticity (Marks et al., 2018). Animals were sedated (butorphanol/dexdomitor cocktail, 0.2 mg/kg), and a transcutaneous electrode was placed on the skin overlying C2 of the cervical spinal cord. The ground electrode was placed adjacent to the stimulating electrode. The stimulation level was established based on the highest current that did not evoke a muscle twitch and was determined for each session and each animal separately (ranged from 2– 5 mA). Electrical stimulation (3 biphasic pulses) followed unilateral acoustic stimulation (10 ms, 8 kHz pure tone bursts of 40 dB above ABR threshold) by 5 ms. Sedation was reversed with atipamezole (2 mg/kg). Bimodal-stimulation was presented for 20 min/day, 5 days a week for 25 days. This treatment protocol attenuates tinnitus in guinea pigs and in humans (Marks et al., 2018). The other groups (ET, ENT, and N) were left alone and did not receive any (sham)-treatment.

Brain processing

After neurophysiological recordings, animals were killed (1 ml Euthasate, intraperitoneal) and transcardially perfused with 100 mL 0.1M phosphate buffered saline (PBS; pH 7.4), followed by 400 mL paraformaldehyde (PFA; 4%) in PBS. Brains were isolated and post-fixed in 4% PFA overnight at 4 °C. The following day, brains were washed in PBS before being transferred to a 30% sucrose solution in PBS for 4–5 days at 4 °C for cryoprotection.

Subsequently, brains were transferred to a 1:1 30% sucrose:Tissue Tek (Sakura, Finetek) solution overnight at 4 °C. Brains were rapidly frozen using dry ice and stored at −20 °C or −80 °C. Four series of 30 μm coronal brainstem sections were collected using a cryostat (Leica, CM 3050S), mounted on glass slides, air dried, and stored at −20°C. A small hole medial to the left CN was made to mark the ipsilateral side of the noise exposure.

Brain immunohistochemistry

To determine expression of VGLUT1 and VGLUT2, brain sections were incubated in blocking solution (PBS with 1% normal goat serum [Jackson ImmunoResearch laboratories, Inc.] and 0.1% Triton-X) for 30 minutes, to prevent non-specific binding of the secondary antibody. Subsequently, sections were incubated for 24h with a primary antibody against VGLUT1 (polyclonal rabbit anti-VGLUT1, diluted 1:1000 in blocking solution; Synaptic Systems, Cat. #135 303) or VGLUT2 (polyclonal rabbit anti-VGLUT2, diluted 1:1000 in blocking solution; Synaptic Systems, Cat. #135 403). The next day, primary antibody binding was visualized by a 2h-incubation with a fluorescent secondary antibody (Alexa Fluor 555-conjugated goat anti-rabbit, diluted 1:500 in blocking solution; Invitrogen). Sections were cover slipped with Fluoromount-G (eBioscience Inc.). To ensure specificity of the detection method, negative controls for the secondary antibody were obtained, in which sections were not treated with the primary antibody. Specificity of the primary antibodies in cochlear nucleus and cerebellar tissue has been shown previously in our lab (Zhou et al., 2007). Positive controls for VGLUT-immunolabeling were performed in the cerebellar cortex (Takamori et al., 2001; Kaneko et al., 2002; Hioki et al., 2003). All procedures were performed at room temperature.

Brain image capture

Immunoreactivity was assessed using a fluorescent microscope (Leica, DMLB). All parameters for capturing the digitized photomicrographs were determined in a pilot study to achieve optimal contrast between labeling and background. Once determined, these parameters were maintained for all subsequent photomicrographs. Exposure times of VGLUT1- and VGLUT2-stained sections were 500 ms and 2500 ms, respectively due to different immunofluorescent intensities, so that final maximum immunofluorescence was equivalent for each antibody. Photomicrographs were taken in each of the major CN subdivisions: the molecular and the deep layers of the dorsal cochlear nucleus (DCN1 and DCN3, respectively), the granule cell domain (GCD), the posteroventral cochlear nucleus (PVCN), and the anteroventral cochlear nucleus (AVCN) (Figure 1). In both CN of each animal, three photomicrographs were taken at equal intervals from caudal to rostral for each of the selected regions (i.e. one picture from the 25^{th} percentile, one from the 50^{th} percentile, and one from the 75^{th} percentile). All pictures were taken at 40X magnification, except VGLUT1-stained DCN1 images, which were taken at 63X magnification in order to capture the multiple small VGLUT1-positive puncta in DCN1 (see Figure 6A).

Brain image analysis

Photomicrographs were processed and analyzed as shown in Figure 2 using Image J (version 1.50a; National Institute of Health, USA). Original RGB images (Figure 2A) were converted to 8-bit images (Figure 2B), after which an automated thresholding paradigm was applied

("*Intermodes Auto Threshold*" for 40X images and "*Bernsen Auto Local Threshold*" for 63X images; Figure 2C). Subsequently, the "*Watershed*" option in Image J separated puncta that appeared fused (Figure 2D). This objective protocol was tested and visually confirmed on VGLUT1 and VGLUT2 images of all regions of the CN to be correctly representing puncta counts, as determined subjectively by two different observers. Puncta counts were determined using the "*Analyze particles*" option in Image J and divided by image area, to yield VGLUT puncta density. Two animals were excluded from the analysis: in one animal, the negative control did not result in negative immunoreactivity; the other animal had a permanent threshold shift.

Cochlear processing

Following transcardial perfusion as described above, the round and oval windows were opened, and fixative was flushed through the scalae. Temporal bones were extracted and post-fixed in 4% PFA for 2h at room temperature, then transferred into 0.12M EDTA, pH 7.0, for decalcification at room temperature. Cochleae were then microdissected, cryoprotected, frozen, thawed, and rinsed in PBS. Immunoprocessing began with a 1h block at room temperature in 5% normal horse serum in PBS and 1% Triton X-100 followed by overnight incubation at 37°C with primary antibodies diluted in 1% normal horse serum with 1% Triton X-100. In all cases, we used 1) mouse (IgG1) anti-CtBP2 (C-terminal Binding Protein) at 1:50 (#612044, BD Transduction Labs) for quantifying pre-synaptic ribbons and 2) rabbit anti- Myosin VIIa at 1:100 (#25–6790 Proteus Biosciences) for counting hair cells. In some cases, we added 1) mouse (IgG2a) anti-GluA2 (glutamate receptor subunit A2) at 1:200 (#MAB397, Millipore) for quantifying post-synaptic receptor patches, 2) chicken anti-neurofilament at 1:1000 (Chemicon, #AB5539) to visualize nerve terminals within the organ of Corti, or 3) goat anti-ChAT (choline acetyl transferase) (Millipore, #AB144P) for quantifying olivocochlear efferents. Cochlear pieces then underwent two, sequential, 60-min incubations at 37°C in species-appropriate secondary antibodies diluted in 1% normal horse serum with 1% Triton X-100: 1) Pacific Blue-conjugated goat anti-rabbit IgG at 1:200 (#P10994, Thermo Fisher); 2) Alexa Fluor 568-conjugated goat anti-mouse (IgG1) at 1:1000 (#A21124, Thermo Fisher); and 3) Alexa Fluor 488-conjugated goat anti-mouse (IgG2a) at 1:500 (#A21131, Thermo Fisher). Epithelial whole mounts were slide-mounted using Vectashield (#H-1000, Vector Labs) then imaged at low magnification to create a cochlear frequency map.

Cochlear synaptic analysis

In each case, the inner hair cell region was imaged at 10 log-spaced frequency regions via confocal microscopy with a glycerol-immersion 63X objective (1.3 N.A.) and 3.2X digital zoom. For each image stack, the z dimension was sampled at 0.25 μm, with the span adjusted to include all synaptic elements in the xy field of view. Each z-stack included ˜8–12 adjacent IHCs, and two contiguous z-stacks were obtained in each frequency location in each ear. Pre-synaptic ribbons in each z-stack were isolated and counted using the "*connected components"* function in Amira, and then divided by the number of IHCs in the stack to compute the mean number of synaptic ribbons per IHC. Prior work with guinea pig ears triple stained for CtBP2, Myosin VIIa, and GluA2 showed that > 96% of all CtBP2-positive ribbon puncta remaining after synaptopathic noise exposure are paired with post-

synaptic glutamate receptor patches (Furman et al., 2013), and are therefore likely functional synapses.

Statistics

To establish statistical significance, two-way ANOVAs, three-way ANOVAs, Tukey-Kramer's post-hoc tests, and Student's T-tests were applied as appropriate. MatLab (The MathWorks, Inc.) was used to analyze and plot the data, and to test for statistical significance (alpha = 0.05).

Results

Tinnitus is not correlated with ABR thresholds, wave 1 amplitudes, or ribbon synapse loss

Twelve weeks after the last noise exposure (t2), ten animals had increased GI ratios (by one-tailed t-test) and were classified with behavioral evidence of tinnitus (ET), whereas nine noise-exposed animals did not have increased GI ratios (by one-tailed t-test) and were classified as having no tinnitus (ENT). Sham exposure did not result in increased GI ratios (by one-tailed t-test). Subsequent treatment in a subgroup of the tinnitus animals (ET_T; n=4) significantly decreased GI ratio (two-tailed t-test of ET vs. ET_T at t3: $T(8) = 2.6$, $p = 0.03$) towards levels comparable to animals without tinnitus (Figure 3A), suggesting that bimodal stimulation treatment reduced tinnitus behavior in these animals. Differences in GI ratios between the animal groups were not associated with changes in Preyer's startle reflex amplitudes, as these were stable throughout the study for all animals (two-way ANOVA: $F(2,2) = 0.01$, $p = 0.99$ for time-point, $F = 0.47$, $p = 0.63$ for group; Figure 3B). Furthermore, when the silent gap in background noise was replaced by a pre-pulse noise burst in a quiet background, none of the noise-exposed animals showed altered pre-pulse inhibition (PPI) ratios (two-way ANOVA: $F(2,2) = 0.81$, $p = 0.45$ for time-point, $F = 0.39$, $p = 0.67$ for group; Figure 3C), indicating that the animals did not have generalized hearing impairment, temporal processing anomalies, or anomalous startle behavior.

Noise exposure induced a mean temporary threshold shift (TTS) of 20 dB immediately following the exposure (three-way ANOVA: factor time point, $F(2,3,1) = 72$, $p = 3.7*10^{-14}$; Figure 4A). There were no significant differences between the TTS of exposed tinnitus (ET), exposed no-tinnitus (ENT), and exposed tinnitus-treated (ET_T) animals (post-hoc Tukey-Kramer's test). Two weeks following noise exposure, thresholds recovered completely for all noise-exposed animals and were similar to thresholds of control animals (N). Thresholds remained normal at 12 weeks post-exposure (post-hoc at tf: $p<0.05$; Figure 4A). The amplitude of ABR wave 1 was reduced following noise exposure (three-way ANOVA: factor time point, $F(5,3,1) = 28$, $p = 2.2*10^{-7}$; Figure 4B). However, there were no differences in amplitudes between the different noise-exposed groups (three-way ANOVA: factor group, $F(5,3,1) = 0.92$, $p = 0.43$).

Consistent with reduced wave 1 amplitudes, ribbon synapses in noise-exposed animals were reduced in number compared to sham-exposed controls in the high-frequency region of the cochlea (examples from the 22.6 kHz are shown in Figure 5). Composite data show that the loss of ribbon synapses in inner hair cells in the noise-exposed animals was modest but

highly significant (two-way ANOVA: factor group, $F(9,3) = 20$, $p = 1.9*10^{-12}$; Figure 4C). As for the wave I reductions, there were no significant differences among the three noise-exposed groups with respect to ribbon synapse loss.

Together, these results suggest that the development and presence of tinnitus was not influenced by the magnitude of the temporary threshold shift or the reduction in suprathreshold wave-1 amplitude, and that the loss of cochlear ribbon synapses was not, in itself, sufficient for the development of tinnitus.

Tinnitus is associated with altered VGLUT1 and VGLUT2 expression in some CN subdivisions

Figure 6 shows typical VGLUT1 immunostaining in each CN subdivision of a control animal. The dense VGLUT1 expression in DCN1 reflects the mostly the VGLUT1-positive parallel-fiber synapses from the granule cells (Fremeau et al., 2001; Hioki et al., 2003; Rubio et al., 2008). VGLUT1 immunoreactivity in DCN3, AVCN, PVCN, and GCD represents primarily auditory-nerve projections and to a lesser extent non-cochlear somatosensory projections (Zhou et al., 2007). The characteristic rings of VGLUT1 puncta in AVCN (Figure 6C) and PVCN (Figure 6D) represent auditory-nerve endbulbs of Held around the spherical and globular bushy cells (Tolbert and Morest, 1982; Ryugo and Sento, 1991).

Mean VGLUT1 puncta density in different subdivisions of the ipsi- and contralateral CN are shown in Figure 7. A two-way ANOVA with factors f1) side and f2) group was calculated for each region. Post-hoc testing showed significant interaural differences in VGLUT1 expression for tinnitus animals, in DCN3 ($f1 = 4.6$, $p = 0.032$; $f2 = 7$, $p = 0.00014$; $f1*f2 = 37$, $p = 0.012$; Figure 7B) and AVCN ($f1 = 3.8$, $p = 0.052$; $f2 = 2.2$, $p = 0.089$; $f1*f2 = 3.7$, $p = 0.012$; Figure 7C). No such interaural differences were seen control, no-tinnitus, or tinnitus-treated animals. An example of asymmetric VGLUT1 density in AVCN from a tinnitus animal is shown in Figure 8A and 8B, where it is compared to a representative exposed no-tinnitus animal in Figure 8C and8D and to a representative exposed tinnitus treated animal in Figure 8E and 8F.

In addition, VGLUT1 density in contralateral DCN3 was significantly lower in tinnitus animals compared to controls (Figure 7B) and was significantly higher in ipsilateral GCD in tinnitus-treated animals compared to the no-tinnitus group ($f1 = 5.6$, $p = 0.018$; $f2 = 7$, $p = 0.00013$, $f1*f2 = 0.49$, $p = 0.69$, Figure 7E). VGLUT1 in ipsilateral and contralateral DCN1 was increased in all noise-exposed animals compared to controls ($f1 = 0.51$, $p = 0.47$; $f2 = 87$, $p = 4.9e\text{-}43$; $f1*f2 = 0.22$, $p = 0.88$, Figure 7A), whereas VGLUT1 in PVCN did not differ between groups or sides ($f1 = 0.25$, $p = 0.62$; $f2 = 0.83$, $p = 0.48$; $f1*f2 = 1.5$, $p = 0.22$; Figure 7D).

Typical VGLUT2 immunostaining is shown in Figure 9 for each CN subdivision of a control animal. VGLUT2 expression throughout the CN represents non-cochlear projections, including those from the somatosensory and vestibular system (Zhou et al., 2007; Zeng et al., 2011; Barker et al., 2012). VGLUT2 immunoreactivity is highest in the GCD, consistent

with a prominent projection from non-cochlear centers to this subdivision (Zhou and Shore, 2004; Haenggeli et al., 2005; Zeng et al., 2011).

VGLUT2 puncta densities in each region of the ipsilateral and contralateral CN are shown in Figure 10. As for VGLUT1 expression, significant differences between ipsilateral and contralateral density were only seen in tinnitus animals. In the AVCN of tinnitus animals, VGLUT2 density was significantly higher ipsilateral than contralateral to the noise ($f1 = 18$, $p = 2.2e-5$; $f2 = 15$, $p = 2.3e-9$; $f1*f2 = 11$, $p = 5.4e-7$, Figure 10C). An example of this ipsilateral upregulation of VGLUT2 is shown in Figure 11A and 11B, compared to a no-tinnitus animal in Figure 11C and 11D and to a tinnitus treated animal in Figure 11E and 11F.

AVCN VGLUT2 was higher in tinnitus as well as no-tinnitus groups compared to the control groups (post-hoc $p < 0.05$) and apparently recovered to control values following bimodal-stimulation treatment (Figure 10C). In the GCD, tinnitus animals showed significantly higher VGLUT2 expression ipsilaterally vs. contralaterally ($f1 = 2.7$, $p = 0.099$; $f2 = 7.4$, $p = 6.8e-5$; $f1*f2 = 2.7$, $p = 0.043$, Figure 10E), and ipsilateral VGLUT2 was higher than controls in both tinnitus and no-tinnitus animals. In the tinnitus animals, that upregulation apparently recovered after bimodal-stimulation treatment (Figure 10E). In DCN1, contralateral VGLUT2 density was increased in tinnitus animals compared to controls ($f1 = 0.075$, $p = 0.78$; $f2 = 6.2$, $p = 0.0004$; $f1*f2 = 0.62$, $p = 0.6$, Figure 10A). No differences were observed in DCN3 ($f1 = 3.1$, $p = 0.08$; $f2 = 1.2$, $p = 0.32$; $f1*f2 = 0.21$, $p = 0.89$; Figure 10B) or PVCN ($f1 = 4.9$, $p = 0.027$; $f2 = 4.5$, $p = 0.0044$; $f1*f2 = 1$, $p = 0.37$; Figure 10D).

These data demonstrate that after mild noise exposure, causing no permanent threshold shift and a mild cochlear synaptopathy, VGLUT1 expression was altered in DCN1, DCN3, AVCN, and GCD, and VGLUT2 expression was altered in DCN1, AVCN, and GCD. Some of these changes appeared regardless of the presence or absence of tinnitus behavior, such as a bilateral upregulation of VGLUT1 in DCN1. The most prominent differences unique to animals showing behavioral evidence of tinnitus were interaural asymmetries in VGLUT expression: VGLUT1 in AVCN and DCN3 driven by contralateral downregulation (Figure 7) and VGLUT2 in AVCN and the GCD driven by ipsilateral upregulation (Figure 10). These tinnitus-specific interaural differences disappeared after the bimodal-stimulation treatment.

Discussion

The current study demonstrated an ipsilateral upregulation of VGLUT2 and an interaural asymmetry in both VGLUT1 and VGLUT2 expression in several CN subdivisions in animals that developed tinnitus. Furthermore, these changes were reversed upon bimodal-stimulation treatment that reduced behavioral and physiological evidence of tinnitus (Marks et al., 2018). Animals with vs. without tinnitus did not differ with respect to measures of cochlear dysfunction or histopathology, including temporary threshold shift, ABR wave-1 amplitude, or ribbon synapse loss.

Tinnitus-related changes in VGLUT2 expression likely reflect upregulated somatosensory-to-CN projections

Tinnitus animals exhibited increased ipsilateral VGLUT2 puncta density in AVCN and GCD compared to the contralateral side and compared to control animals, indicating a higher density of VGLUT2-positive pre-synaptic terminals in these subdivisions. This finding is consistent with studies in guinea pig and mouse showing ipsilateral VGLUT2 puncta density increases following cochlear damage (Zeng et al., 2009; Heeringa et al., 2016). Axonal sprouting, i.e. the formation of new synapses, from other noncochlear areas is a likely underlying mechanism for the increased VGLUT2 puncta density. Axonal sprouting in cochlear nucleus has been shown to occur following acoustic trauma (Bilak et al., 1997; Kim et al., 2004a). Electron microscopic analysis shows that these newly-grown axons are qualitatively different from auditory nerve synapses and are likely derived centrally (Kim et al., 2004b). Furthermore, several markers for axonal outgrowth and synaptic sprouting, including GAP-43 (Benowitz and Routtenberg, 1997), glial fibrillary acidic protein (GFAP) (Brenner, 2014), and synaptophysin (Leclerc et al., 1989), have been shown to be increased following acoustic trauma or salicylate treatment (Muly et al., 2002; Kraus et al., 2011; Fang et al., 2016). Previous research showed that the number of somatosensory terminals from the spinal trigeminal nucleus and cuneate nucleus to the CN increases following cochlear damage, and that these projections are VGLUT2-positive (Zeng et al., 2012). Zeng et al demonstrated that changes in VGLUT2 puncta density correlated with changes in number of terminals from the somatosensory system following cochlear damage. In tinnitus animals, upregulation of VGLUT2 puncta density was confined to the AVCN and GCD, which is consistent with the locations where projections from the spinal trigeminal nucleus and the cuneate nucleus were increased following cochlear damage (Zeng et al., 2012). Barker et al. (2012) also showed increases in VGLUT2-positive projections from the lateral vestibular nucleus to the DCN after noise exposure (Barker et al., 2012). It is therefore likely that the tinnitus-related increases in ipsilateral VGLUT2 density are similarly due to an upregulation of non-cochlear innervation derived from somatosensory and perhaps also vestibular brainstem regions (Barker et al., 2012; Zeng et al., 2012).

Furthermore, the bimodal-stimulation treatment specifically targeted the somatosensory system by activating the C2 and dorsal column pathways to the GCD (Wu et al., 2015). The treatment reversed the increased VGLUT2 puncta density and VGLUT asymmetries in tinnitus animals further supporting the contention that the tinnitus-related changes in glutamatergic projections to the CN are related to an upregulation of somatosensory projections to the CN.

Correspondingly, neurophysiological studies have shown that auditory-somatosensory plasticity is altered in an animal model of tinnitus. In fusiform cells of tinnitus animals, the prevalence of excitatory responses to unimodal stimulation of the spinal trigeminal nucleus increases while inhibitory responses decrease, and long-term potentiation is increased upon bimodal auditory-somatosensory stimulation (Dehmel et al., 2012; Koehler and Shore, 2013). These responses likely reflect the pathophysiology seen in fusiform cells of animals with behavioral correlates of tinnitus, including increased spontaneous firing rate, increased synchrony, and increased bursting activity (Brozoski et al., 2002; Kaltenbach et al., 2004;

Wu et al., 2016a). Bimodal-stimulation treatment reduces both synchrony and spontaneous activity in the same tinnitus animals that were used in the current study (Marks et al., 2018), suggesting that glutamatergic redistribution of somatosensory projections is associated with the long-term changes in DCN neuronal activity that accompany tinnitus.

It remains possible that the puncta density changes partly reflect synaptic density changes, i.e. the amount of VGLUT at the synapse reduces to such a low number that it could not be detected. However, the effects on the neurophysiological outcomes, as described above, remain the same. Furthermore, it is unlikely that an ipsilateral CN volume decrease in tinnitus animals confounded the results. First, the magnitudes of the puncta density changes, along with previous research showing no more than a 10–25% volume decrease following more severe cochlear trauma (Kraus et al., 2011; Kurioka et al., 2016), suggests that an ipsilateral volume reduction to half its size or a contralateral volume increase to more than twice its size is highly unlikely. Second, if volume changes were an underlying mechanism of the changes in puncta density, there would have been similar outcomes for VGLUT1 and VGLUT2 changes, which was not the case. In summary, we conclude that the tinnitus-related ipsilateral VGLUT2 puncta density increases likely reflect upregulation of non-cochlear terminals to the CN.

Tinnitus-related changes in VGLUT1 expression may be related to a tonically-activated olivocochlear pathway

Previous studies suggest that the cochlear damage-induced upregulation of noncochlear, VGLUT2-positive projections was triggered by a downregulation of VGLUT1-positive input from the auditory nerve, i.e. an auditory-somatosensory redistribution (Zeng et al., 2009; Barker et al., 2012; Zeng et al., 2012; Heeringa et al., 2016). However, here we show that ipsilateral VGLUT1 puncta density was not affected by a mild noise exposure, suggesting that the tinnitus-related noncochlear upregulation was not triggered by a loss of synaptic auditory nerve input. This is consistent with the absence of tinnitus-specific changes in the cochlear measures reported here. Temporary threshold shifts, followed by permanent reductions of ABR wave-1 amplitudes and ribbon synapse counts were observed in all noise-exposed animals, including animals that did not develop behavioral evidence of tinnitus. However, some of the ipsilateral VGLUT1-positive auditory nerve synapses may have been “silenced” (i.e. no longer transmitting any information from the cochlea) due to a noise-induced loss of ribbon synapses in the cochlea and were not able to compete with sprouting of non-cochlear projections in the tinnitus animals.

The no-tinnitus animals did not show glutamatergic asymmetries, while those with tinnitus demonstrated interaural asymmetries for VGLUT1 density in DCN3 and AVCN, regions that both receive a substantial innervation from the auditory nerve (Zhou et al., 2007). However, in both regions, a contralateral downregulation of VGLUT1 was responsible for the asymmetry, rather than an ipsilateral upregulation (Figure 7C). There was a similar, but not significant, trend of interaural asymmetry in VGLUT1 density in the PVCN and GCD of tinnitus animals, which was not seen in sham-exposed, no-tinnitus, or tinnitus-treated animals. This finding is consistent with previous research showing that contralateral glutamate receptors in the CN can be affected by ipsilateral conductive hearing loss.

Together with the current study, this shows evidence of plasticity in glutamatergic synapses following changes in auditory nerve activity on the opposite side (Whiting et al., 2009). Contralateral VGLUT1 downregulation could be explained by tinnitus-related hyperactivity in the ipsilateral VCN (Bledsoe et al., 2009; Vogler et al., 2011; Gu et al., 2012), which could tonically activate the medial olivocochlear pathway (de Venecia et al., 2005), suppressing the output of the contralateral cochlea and in turn reducing the activation of the contralateral DCN3 and AVCN. Furthermore, medial olivocochlear neurons have branches that project to the granule cell region and dorsal and ventral cochlear nucleus (Brown, 1993; Baashar et al., 2015), which may influence the plasticity of granule-cell axonal synapses with the apical dendrites of fusiform cells (Marks et al., 2018). Furthermore, tinnitus-related disruptions in the lateral superior olive could also have been involved in a contralateral downregulation of VGLUT1, resulting in the observed asymmetry in VGLUT1 puncta density. Importantly, no-tinnitus animals and tinnitus-treated animals, exposed to the same noise, showed the same cochlear histopathology and dysfunction, yet did not exhibit interaural asymmetries in VGLUT1 density in the DCN3 and AVCN. This indicates that the glutamatergic asymmetry is tinnitus specific.

VGLUT1 density in DCN1 was increased in both CNs for all noise-exposed animals suggesting that the parallel fiber synapses from granule cells (Fremeau et al., 2001; Hioki et al., 2003; Rubio et al., 2008), which receive non-cochlear projections (Wright and Ryugo, 1996; Ryugo et al., 2003), are increased irrespective of whether the animal exhibits tinnitus behavior. Parallel fibers synapse onto the apical dendrites of fusiform cells, the DCN principal output neurons, and onto cartwheel cells, the DCN inhibitory interneurons (Golding and Oertel, 1997; Tzounopoulos et al., 2004). Since bimodal plasticity, which requires the parallel fiber synapses (Tzounopoulos et al., 2004), is remarkably different between tinnitus and no-tinnitus animals (Koehler and Shore, 2013; Marks et al., 2018), it is likely that the upregulated parallel fiber synapses differentially target fusiform cells vs. their inhibitory interneurons, the cartwheel cells, in animals with vs. without tinnitus. If this were indeed the case, bimodal stimulation treatment would then alter the target cells of the upregulated parallel fiber synapses to reverse tinnitus.

Implications

Studies focusing on inhibitory neurotransmission in the CN demonstrated that tinnitus correlates with plasticity at glycinergic synapses and with decreased GABAergic neurotransmission in the DCN (Wang et al., 2009; Middleton et al., 2011). Although it has been speculated that glutamatergic inputs are altered in tinnitus (Barker et al., 2012; Zeng et al., 2012; Koehler and Shore, 2013), this is the first study providing direct evidence that markers of excitatory neurotransmission (Takamori et al., 2000, 2001) are redistributed in animals with a behavioral manifestation of tinnitus. Previous studies have shown that increases in pre-synaptic VGLUTs correspond to an increase in the amount of glutamate release and are associated with EPSCs of higher amplitude and lower failure rate in the postsynaptic cell (Wilson et al., 2005; Moechars et al., 2006). Thus, increases in VGLUT expression in the current study likely reflect increased glutamate release and likely precede the tinnitus-specific increases in ipsilateral DCN spontaneous activity, synchrony and long-

term potentiation in tinnitus (Wu et al., 2016a; Wu et al., 2016b), despite the reductions in ipsilateral auditory nerve activity due to the noise-induced synaptic damage.

Temporary threshold shifts, followed by permanent reductions of ABR wave-1 amplitudes and ribbon synapse counts were observed in all noise-exposed animals. In contrast, VGLUT asymmetry between the CNs was specific for animals with a behavioral manifestation of tinnitus. This is consistent with studies suggesting that the CN is the first site along the auditory pathway of tinnitus generation (Shore et al., 2016; Wu et al., 2016a; Guest et al., 2017). It remains possible that reduction in auditory nerve activation of the CN after cochlear synaptopathy is necessary but not sufficient for subsequent tinnitus generation after noise exposure.

In summary, our results show that tinnitus is associated with an ipsilateral upregulation of VGLUT2-positive projections that likely derive from somatosensory projections to the GCD and AVCN. This upregulation may underlie the neurophysiological hallmarks of tinnitus in the DCN. Furthermore, bimodal auditory-somatosensory stimulation treatment reverses the tinnitus-associated changes in glutamatergic projections, emphasizing the relevance of CN plasticity in tinnitus.

Acknowledgements

The authors thank Sarah Koslakiewicz, James Wiler, and Ariane Kanicki for technical assistance.

This research was funded by NIH R01-DC004825 (SES), NIH P30-DC05188, NIH T32-DC00011, NIH DC 00188 (MCL), the Coulter Foundation, and the generous support of Tom and Helene Lauer.

Abbreviations

ABR	auditory brainstem response
AVCN	anteroventral cochlear nucleus
CN	cochlear nucleus
DCN	dorsal cochlear nucleus
DCN1	molecular layer of the dorsal cochlear nucleus
DCN3	deep layer of the dorsal cochlear nucleus
ET	exposed tinnitus
ENT	exposed no tinnitus
ET_T	exposed tinnitus treated
GCD	granule cell domain
GI	gap index
GPIAS	gap-pre pulse inhibition of the acoustic startle reflex
icp	inferior cerebellar peduncle

N	sham-exposed control animals
PBS	phosphate buffered saline
PFA	paraformaldehyde
PVCN	posteroventral cochlear nuclues
Sp5	spinal trigeminal nucleus
sp5	spinal trigeminal tract
TTS	temporary threshold shift
tz	trapezoid body
VCN	ventral cochlear nucleus
VGLUT1	vesicular glutamate transporter 1
VGLUT2	vesicular glutamate transporter 2

References

Baashar A, Robertson D, Mulders WH (2015) A novel method for selectively labelling olivocochlear collaterals in the rat. Hear Res 325:35–41. [PubMed: 25814172]

Barker M, Solinski HJ, Hashimoto H, Tagoe T, Pilati N, Hamann M (2012) Acoustic overexposure increases the expression of VGLUT-2 mediated projections from the lateral vestibular nucleus to the dorsal cochlear nucleus. PLoS One 7:e35955. [PubMed: 22570693]

Benowitz LI, Routtenberg A (1997) GAP-43: an intrinsic determinant of neuronal development and plasticity. Trends Neurosci 20:84–91. [PubMed: 9023877]

Berger JI, Coomber B, Shackleton TM, Palmer AR, Wallace MN (2013) A novel behavioural approach to detecting tinnitus in the guinea pig. Journal of neuroscience methods 213:188–195. [PubMed: 23291084]

Bhatt JM, Lin HW, Bhattacharyya N (2016) Prevalence, Severity, Exposures, and Treatment Patterns of Tinnitus in the United States. JAMA Otolaryngol Head Neck Surg 142:959–965. [PubMed: 27441392]

Bilak M, Kim J, Potashner SJ, Bohne BA, Morest DK (1997) New growth of axons in the cochlear nucleus of adult chinchillas after acoustic trauma. Exp Neurol 147:256–268. [PubMed: 9344551]

Bledsoe SC, Jr., Koehler S, Tucci DL, Zhou J, Le Prell C, Shore SE(2009) Ventral cochlear nucleus responses to contralateral sound are mediated by commissural and olivocochlear pathways. J Neurophysiol 102:886–900. [PubMed: 19458143]

Brenner M (2014) Role of GFAP in CNS injuries. Neurosci Lett 565:7–13. [PubMed: 24508671]

Brown MC (1993) Fiber pathways and branching patterns of biocytin-labeled olivocochlear neurons in the mouse brainstem. J Comp Neurol 337:600–613. [PubMed: 8288773]

Brozoski TJ, Bauer CA, Caspary DM (2002) Elevated fusiform cell activity in the dorsal cochlear nucleus of chinchillas with psychophysical evidence of tinnitus. J Neurosci 22:2383–2390. [PubMed: 11896177]

de Venecia RK, Liberman MC, Guinan JJ, Jr., Brown MC (2005) Medial olivocochlear reflex interneurons are located in the posteroventral cochlear nucleus: a kainic acid lesion study in guinea pigs. J Comp Neurol 487:345–360. [PubMed: 15906311]

Dehmel S, Pradhan S, Koehler S, Bledsoe S, Shore S (2012) Noise overexposure alters long-term somatosensory-auditory processing in the dorsal cochlear nucleus--possible basis for tinnitus-related hyperactivity? J Neurosci 32:1660–1671. [PubMed: 22302808]

Eggermont JJ, Roberts LE (2015) Tinnitus: animal models and findings in humans. Cell Tissue Res 361:311–336. [PubMed: 25266340]

Fang L, Fu Y, Zhang TY (2016) Salicylate-Induced Hearing Loss Trigger Structural Synaptic Modifications in the Ventral Cochlear Nucleus of Rats via Medial Olivocochlear (MOC) Feedback Circuit.Neurochem Res 41:1343–1353. [PubMed: 26886762]

Fremeau RT, Jr, Troyer MD, Pahner I, Nygaard GO, Tran CH, Reimer RJ, Bellocchio EE, Fortin D, Storm-Mathisen J, Edwards RH (2001) The expression of vesicular glutamate transporters defines two classes of excitatory synapse. Neuron 31:247–260. [PubMed: 11502256]

Fremeau RT, Jr., Burman J, Qureshi T, Tran CH, Proctor J, Johnson J, Zhang H, Sulzer D, Copenhagen DR, Storm-Mathisen J, Reimer RJ, Chaudhry FA, Edwards RH (2002) The identification of vesicular glutamate transporter 3 suggests novel modes of signaling by glutamate. Proc Natl Acad Sci U S A 99:14488–14493. [PubMed: 12388773]

Furman AC, Kujawa SG, Liberman MC (2013) Noise-induced cochlear neuropathy is selective for fibers with low spontaneous rates. J Neurophysiol 110:577–586. [PubMed: 23596328]

Golding NL, Oertel D (1997) Physiological identification of the targets of cartwheel cells in the dorsal cochlear nucleus. J Neurophysiol 78:248–260. [PubMed: 9242277]

Gu JW, Herrmann BS, Levine RA, Melcher JR (2012) Brainstem auditory evoked potentials suggest a role for the ventral cochlear nucleus in tinnitus. J Assoc Res Otolaryngol 13:819–833. [PubMed: 22869301]

Guest H, Munro KJ, Prendergast G, Howe S, Plack CJ (2017) Tinnitus with a normal audiogram: Relation to noise exposure but no evidence for cochlear synaptopathy. Hear Res 344:265–274. [PubMed: 27964937]

Haenggeli CA, Pongstaporn T, Doucet JR, Ryugo DK (2005) Projections from the spinal trigeminal nucleus to the cochlear nucleus in the rat. J Comp Neurol 484:191–205. [PubMed: 15736230]

Heeringa AN, Stefanescu RA, Raphael Y, Shore SE (2016) Altered vesicular glutamate transporter distributions in the mouse cochlear nucleus following cochlear insult. Neuroscience 315:114– 124. [PubMed: 26705736]

Hioki H, Fujiyama F, Taki K, Tomioka R, Furuta T, Tamamaki N, Kaneko T (2003) Differential distribution of vesicular glutamate transporters in the rat cerebellar cortex. Neuroscience 117:1–6. [PubMed: 12605886]

Kaltenbach JA, Zacharek MA, Zhang J, Frederick S (2004) Activity in the dorsal cochlear nucleus of hamsters previously tested for tinnitus following intense tone exposure. Neurosci Lett 355:121–125. [PubMed: 14729250]

Kaneko T, Fujiyama F, Hioki H (2002) Immunohistochemical localization of candidates for vesicular glutamate transporters in the rat brain. J Comp Neurol 444:39–62. [PubMed: 11835181]

Kim JJ, Gross J, Morest DK, Potashner SJ (2004a) Quantitative study of degeneration and new growth of axons and synaptic endings in the chinchilla cochlear nucleus after acoustic overstimulation. J Neurosci Res 77:829–842. [PubMed: 15334601]

Kim JJ, Gross J, Potashner SJ, Morest DK (2004b) Fine structure of long-term changes in the cochlear nucleus after acoustic overstimulation: chronic degeneration and new growth of synaptic endings. J Neurosci Res 77:817–828. [PubMed: 15334600]

Koehler S, Shore S (2013) Stimulus Timing-Dependent Plasticity in Dorsal Cochlear Nucleus Is Altered in Tinnitus. Journal of Neuroscience 33:19647–19656. [PubMed: 24336728]

Kraus KS, Ding D, Jiang H, Lobarinas E, Sun W, Salvi RJ (2011) Relationship between noise-induced hearing-loss, persistent tinnitus and growth-associated protein-43 expression in the rat cochlear nucleus: does synaptic plasticity in ventral cochlear nucleus suppress tinnitus? Neuroscience 194:309–325. [PubMed: 21821100]

Kurioka T, Lee MY, Heeringa AN, Beyer LA, Swiderski DL, Kanicki AC, Kabara LL, Dolan DF, Shore SE, Raphael Y (2016) Selective hair cell ablation and noise exposure lead to different patterns of changes in the cochlea and the cochlear nucleus. Neuroscience 332:242–257. [PubMed: 27403879]

Leclerc N, Beesley PW, Brown I, Colonnier M, Gurd JW, Paladino T, Hawkes R (1989) Synaptophysin expression during synaptogenesis in the rat cerebellar cortex. J Comp Neurol 280:197–212. [PubMed: 2494237]

Levine RA (1999) Somatic (craniocervical) tinnitus and the dorsal cochlear nucleus hypothesis. Am J Otolaryngol 20:351–362. [PubMed: 10609479]

Marks KL, Martel DT, Wu C, Basura GJ, Roberts LE, Schvartz-Leyzac KC, Shore SE (2018) Auditory-somatosensory bimodal stimulation desynchronizes brain circuitry to reduce tinnitus in guinea pigs and humans. Sci Transl Med 10.

Middleton JW, Kiritani T, Pedersen C, Turner JG, Shepherd GM, Tzounopoulos T (2011) Mice with behavioral evidence of tinnitus exhibit dorsal cochlear nucleus hyperactivity because of decreased GABAergic inhibition. Proc Natl Acad Sci U S A 108:7601–7606. [PubMed: 21502491]

Moechars D, Weston MC, Leo S, Callaerts-Vegh Z, Goris I, Daneels G, Buist A, Cik M, van der Spek P, Kass S, Meert T, D'Hooge R, Rosenmund C, Hampson RM (2006) Vesicular glutamate transporter VGLUT2 expression levels control quantal size and neuropathic pain. J Neurosci 26:12055–12066. [PubMed: 17108179]

Muly SM, Gross JS, Morest DK, Potashner SJ (2002) Synaptophysin in the cochlear nucleus following acoustic trauma. Exp Neurol 177:202–221. [PubMed: 12429223]

Ostermann K, Lurquin P, Horoi M, Cotton P, Herve V, Thill MP (2016) Somatic tinnitus prevalence and treatment with tinnitus retraining therapy. B-Ent 12:59–65. [PubMed: 27097395]

Rubio ME, Gudsnuk KA, Smith Y, Ryugo DK (2008) Revealing the molecular layer of the primate dorsal cochlear nucleus. Neuroscience 154:99–113. [PubMed: 18222048]

Ryugo DK, Sento S (1991) Synaptic connections of the auditory nerve in cats: relationship between endbulbs of held and spherical bushy cells. J Comp Neurol 305:35–48. [PubMed: 2033123]

Ryugo DK, Haenggeli CA, Doucet JR (2003) Multimodal inputs to the granule cell domain of the cochlear nucleus. Exp Brain Res 153:477–485. [PubMed: 13680048]

Sanchez TG, Guerra GC, Lorenzi MC, Brandao AL, Bento RF (2002) The influence of voluntary muscle contractions upon the onset and modulation of tinnitus. Audiology & neuro-otology 7:370–375. [PubMed: 12401968]

Shore SE, Roberts LE, Langguth B (2016) Maladaptive plasticity in tinnitus--triggers, mechanisms and treatment. Nat Rev Neurol 12:150–160. [PubMed: 26868680]

Takamori S, Rhee JS, Rosenmund C, Jahn R (2000) Identification of a vesicular glutamate transporter that defines a glutamatergic phenotype in neurons. Nature 407:189–194. [PubMed: 11001057]

Takamori S, Rhee JS, Rosenmund C, Jahn R (2001) Identification of differentiation-associated brain-specific phosphate transporter as a second vesicular glutamate transporter (VGLUT2). J Neurosci 21:RC182. [PubMed: 11698620]

Tolbert LP, Morest DK (1982) The neuronal architecture of the anteroventral cochlear nucleus of the cat in the region of the cochlear nerve root: Golgi and Nissl methods. Neuroscience 7:3013–3030. [PubMed: 6186942]

Tsuji J, Liberman MC (1997) Intracellular labeling of auditory nerve fibers in guinea pig: central and peripheral projections. J Comp Neurol 381:188–202. [PubMed: 9130668]

Turner JG, Brozoski TJ, Bauer CA, Parrish JL, Myers K, Hughes LF, Caspary DM (2006) Gap detection deficits in rats with tinnitus: a potential novel screening tool. Behav Neurosci 120:188–195. [PubMed: 16492129]

Tzounopoulos T, Kim Y, Oertel D, Trussell LO (2004) Cell-specific, spike timing-dependent plasticities in the dorsal cochlear nucleus. Nat Neurosci 7:719–725. [PubMed: 15208632]

Vogler DP, Robertson D, Mulders WH (2011) Hyperactivity in the ventral cochlear nucleus after cochlear trauma. J Neurosci 31:6639–6645. [PubMed: 21543592]

Wang H, Brozoski TJ, Turner JG, Ling L, Parrish JL, Hughes LF, Caspary DM (2009) Plasticity at glycinergic synapses in dorsal cochlear nucleus of rats with behavioral evidence of tinnitus. Neuroscience 164:747–759. [PubMed: 19699270]

Whiting B, Moiseff A, Rubio ME (2009) Cochlear nucleus neurons redistribute synaptic AMPA and glycine receptors in response to monaural conductive hearing loss. Neuroscience 163:1264–1276. [PubMed: 19646510]

Wilson NR, Kang J, Hueske EV, Leung T, Varoqui H, Murnick JG, Erickson JD, Liu G (2005) Presynaptic regulation of quantal size by the vesicular glutamate transporter VGLUT1. J Neurosci 25:6221– 6234. [PubMed: 15987952]

Wright DD, Ryugo DK (1996) Mossy fiber projections from the cuneate nucleus to the cochlear nucleus in the rat. J Comp Neurol 365:159–172. [PubMed: 8821448]

Wu C, Martel DT, Shore SE (2015) Transcutaneous induction of stimulus-timing-dependent plasticity in dorsal cochlear nucleus. Front Syst Neurosci 9:116. [PubMed: 26321928]

Wu C, Martel DT, Shore SE (2016a) Increased Synchrony and Bursting of Dorsal Cochlear Nucleus Fusiform Cells Correlate with Tinnitus. J Neurosci 36:2068–2073. [PubMed: 26865628]

Wu C, Stefanescu RA, Martel DT, Shore SE (2016b) Tinnitus: Maladaptive auditory-somatosensory plasticity. Hear Res 334:20–29. [PubMed: 26074307]

Zeng C, Shroff H, Shore SE (2011) Cuneate and spinal trigeminal nucleus projections to the cochlear nucleus are differentially associated with vesicular glutamate transporter-2. Neuroscience 176:142–151. [PubMed: 21167260]

Zeng C, Nannapaneni N, Zhou J, Hughes LF, Shore S (2009) Cochlear damage changes the distribution of vesicular glutamate transporters associated with auditory and nonauditory inputs to the cochlear nucleus. J Neurosci 29:4210–4217. [PubMed: 19339615]

Zeng C, Yang Z, Shreve L, Bledsoe S, Shore S (2012) Somatosensory projections to cochlear nucleus are upregulated after unilateral deafness. J Neurosci 32:15791–15801. [PubMed: 23136418]

Zhou J, Shore S (2004) Projections from the trigeminal nuclear complex to the cochlear nuclei: a retrograde and anterograde tracing study in the guinea pig. J Neurosci Res 78:901–907. [PubMed: 15495211]

Zhou J, Nannapaneni N, Shore S (2007) Vesicular glutamate transporters 1 and 2 are differentially associated with auditory nerve and spinal trigeminal inputs to the cochlear nucleus. J Comp Neurol 500:777–787. [PubMed: 17154258]

Highlights

- VGLUT2 puncta density is upregulated in the cochlear nucleus ipsilateral to acoustic trauma
- VGLUT1 puncta density is downregulated in the cochlear nucleus contralateral to acoustic trauma
- Tinnitus does not correlate with measures of cochlear dysfunction or histopathology
- VGLUT asymmetries are abolished upon auditory-somatosensory bimodal stimulation treatment that reversed behavioral tinnitus
- Tinnitus-associated glutamatergic redistribution is likely the result of maladaptive somatosensory compensation

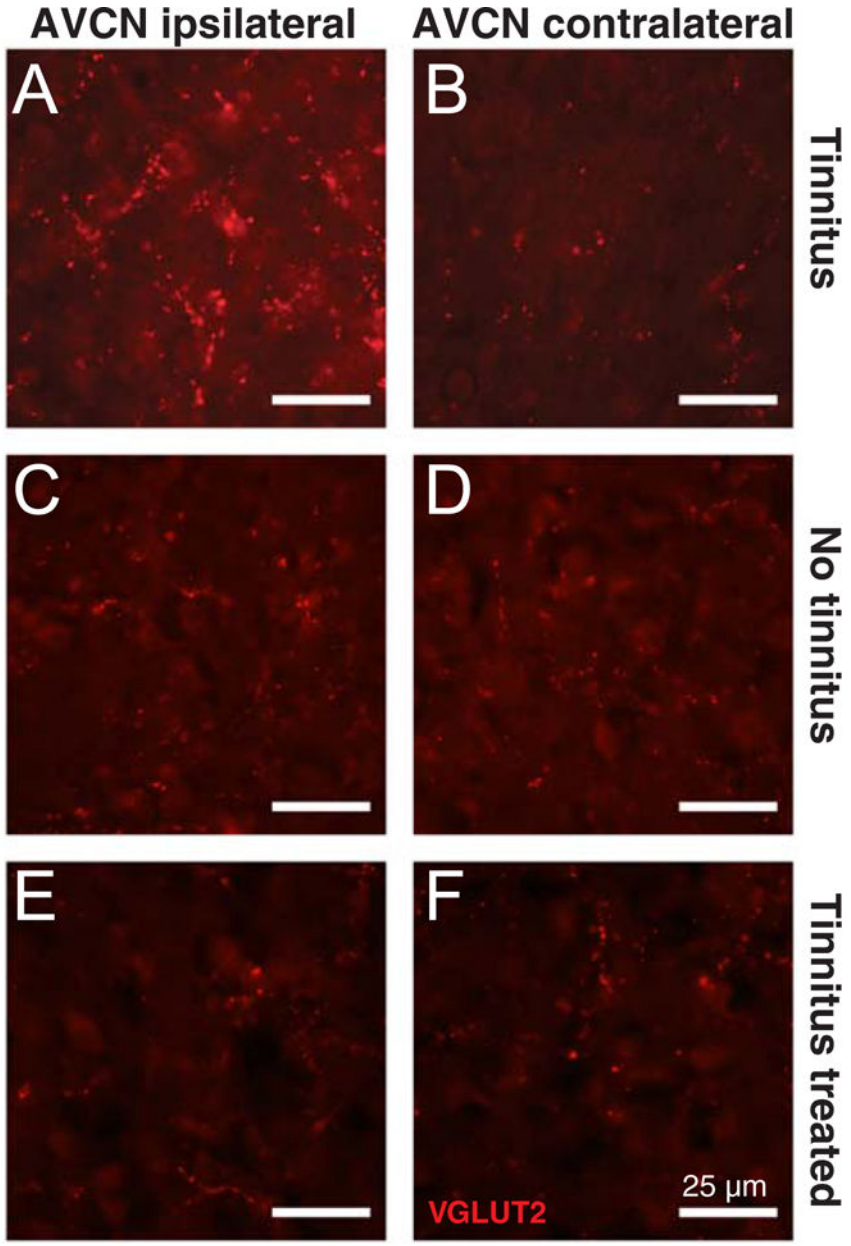

Figure 1: Schematic overview of the CN regions studied.

Transverse sections of the CN from rostral to caudal in panel A-D, respectively, indicate the locations where photomicrographs were taken in the different CN regions used in the current study. DCN1, molecular layer of the dorsal cochlear nucleus; DCN3, deep layer of the dorsal cochlear nucleus; PVCN, posteroventral cochlear nucleus; AVCN, anteroventral cochlear nucleus; GCD, granule cell domain; icp, inferior cerebellar peduncle; sp5, spinal trigeminal tract; tz, trapezoid body.

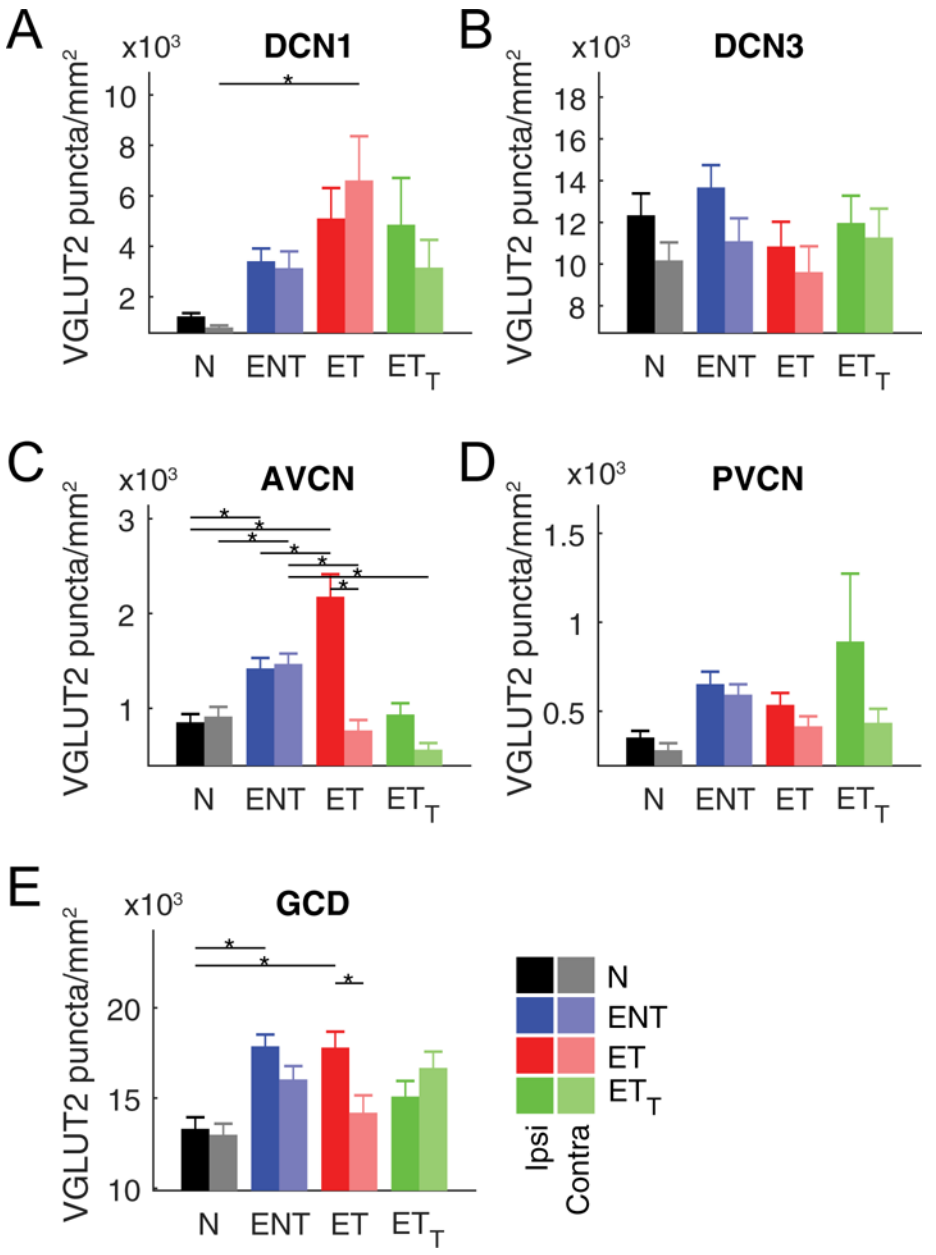

Figure 2: The procedure to count puncta in VGLUT1 and VGLUT2 photomicrographs.

A) Example of an original RGB image from a VGLUT1 staining of the AVCN. B) The photomicrograph from panel A converted to an 8-bit greyscale image. C) Applying the automated thresholding algorithm *Intermodes* (ImageJ) on the image in panel B. D) Applying the *Water-shed* algorithm (ImageJ) on the image in panel C yields a separation of the puncta that were "melted together". The scale bar represents 15 μm and is the same for all panels.

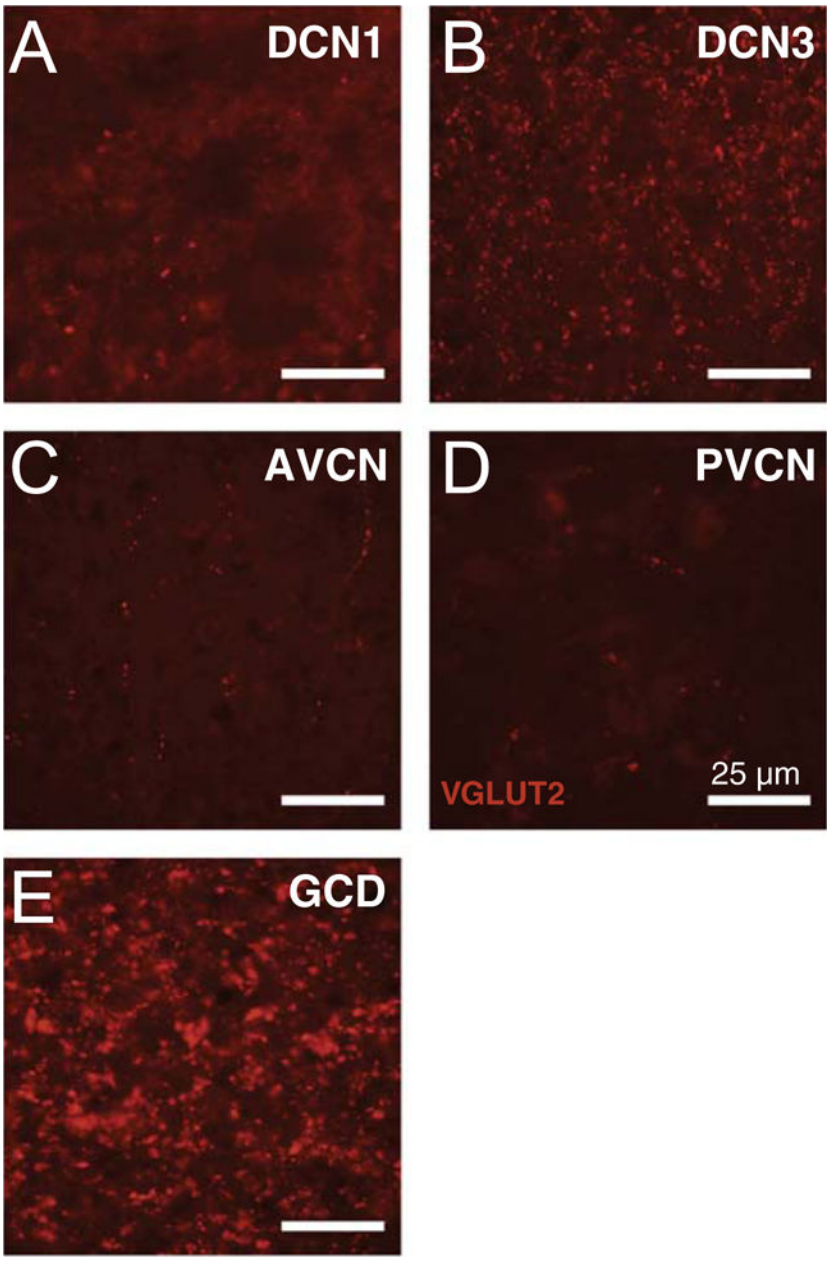

Figure 3: Tinnitus assessment using GPIAS.

A) The top panel shows a schematic of the experimental setup. Guinea pigs were either sham-exposed (control; N) or noise-exposed at t1 after baseline GPIAS testing at t0. GPIAS was tested again at 8 weeks post-exposure, or t2. Exposed-tinnitus animals (ET) were separated from exposed-no-tinnitus animals (ENT) based on significant increases in gap-inhibition (GI) ratio (†; $P<0.05$ *a priori*). A subset of ET animals was treated with bimodal stimulation (reassigned as ET_T). GPIAS was tested again 4 weeks later, tf, before histology. B) Absolute pinna startle amplitude measured for the no gap/pre-pulse trials. No difference was observed between time points or groups. C) Pre-pulse inhibition (PPI) ratio, likewise, did not change throughout the study duration for any of the groups.

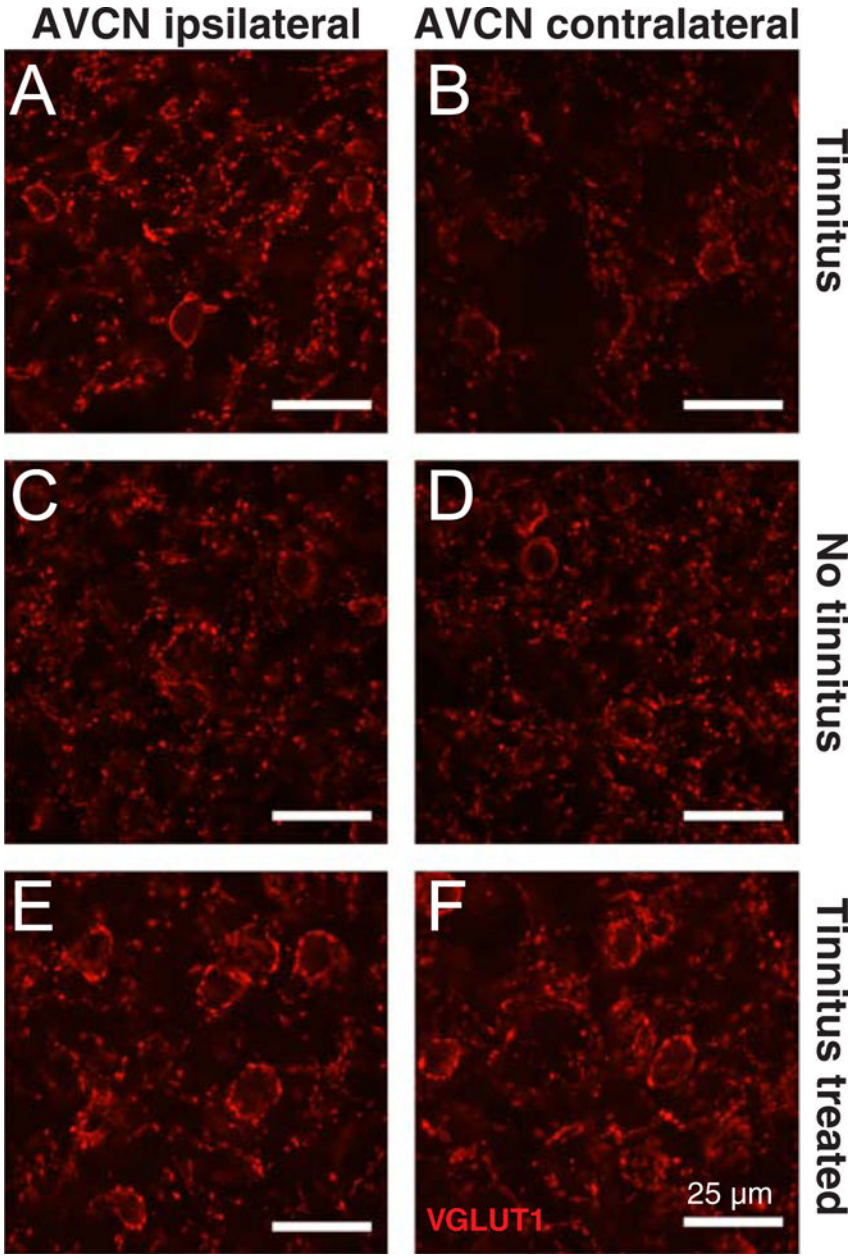

Figure 4: Measures of cochlear pathophysiology and histopathology did not differ between tinnitus and no-tinnitus animals.

A) ABR threshold shifts immediately following noise exposure (t1, solid lines) and 12 weeks following noise exposure (tf, dashed lines). B) ABR wave-1 amplitude (P1-N1) before (t0, solid lines) and 12 weeks after noise exposure (tf, dashed lines). C) Synaptic ribbon counts per IHC, as sampled at 10 locations along the cochlear spiral, converted to frequency according to a published map (Tsuji and Liberman, 1997). Exposed-tinnitus (then treated) animals (ET_T) are in green, exposed tinnitus (untreated) animals (ET) are in red, exposed no-tinnitus animals (ENT) are in blue, and sham-exposed normals (N) are in black for all three panels.

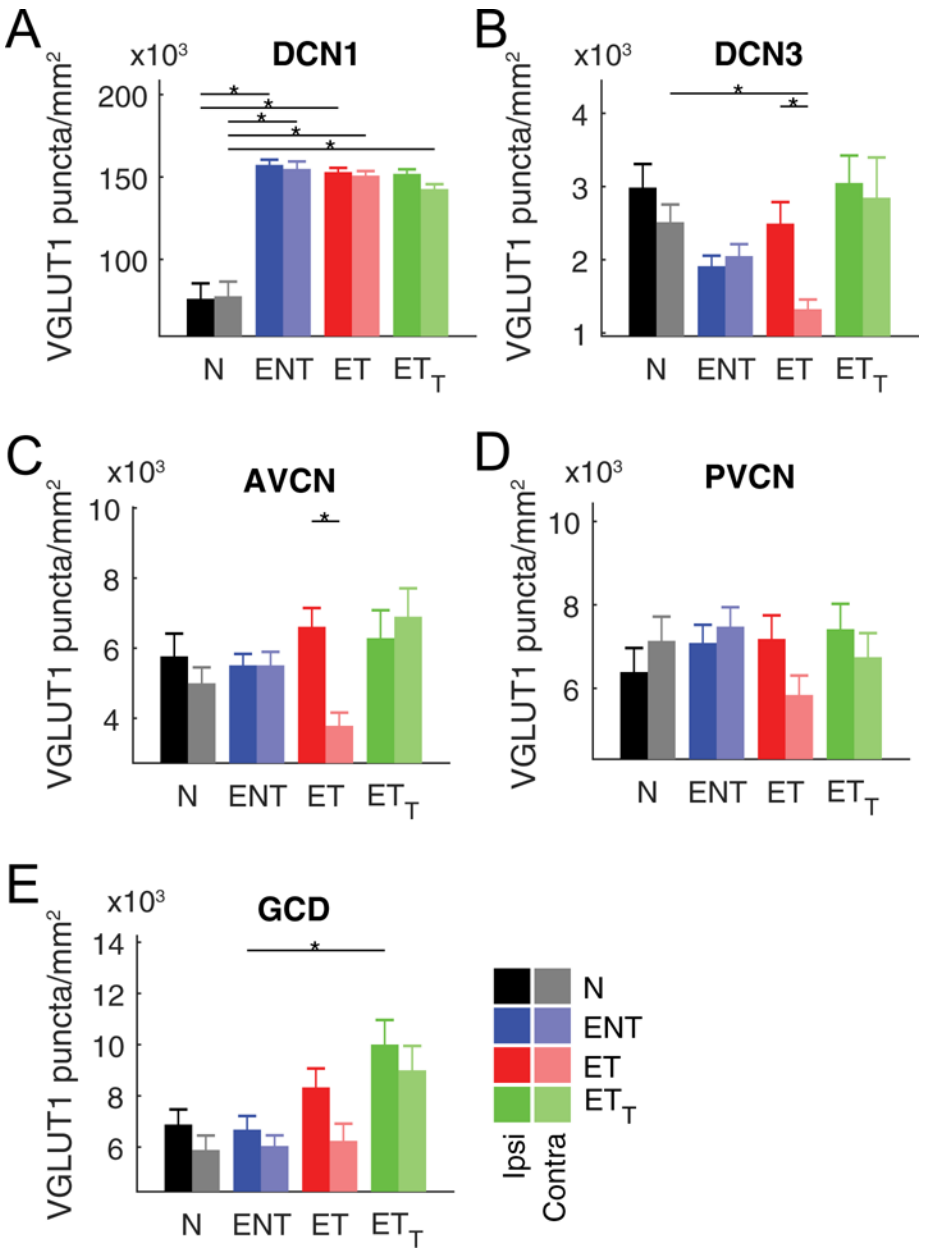

Figure 5: Confocal images of inner hair cells from a control (A) and an exposed ear (B).

Images were immunostained to reveal synaptic ribbons (red - CtBP2), nerve terminals (green - neurofilament), efferent fibers (blue - choline acetyl transferase) and hair cells (white - myosin VIIa). A1, B1: maximum projections in the acquisition plane of 8 or 9 adjacent hair cells. A2, B2: the same confocal z-stacks as in A1 and B2, rotated to view as maximum projections in the yz plane. Both image stacks were from the 22.6 kHz region, from opposite ears in the same animal. There were, on average, 17.37 synaptic ribbons per IHC in panel A and 10.27 synaptic ribbons per IHC in panel B. In each image, the outer hair cell area would be towards the right.

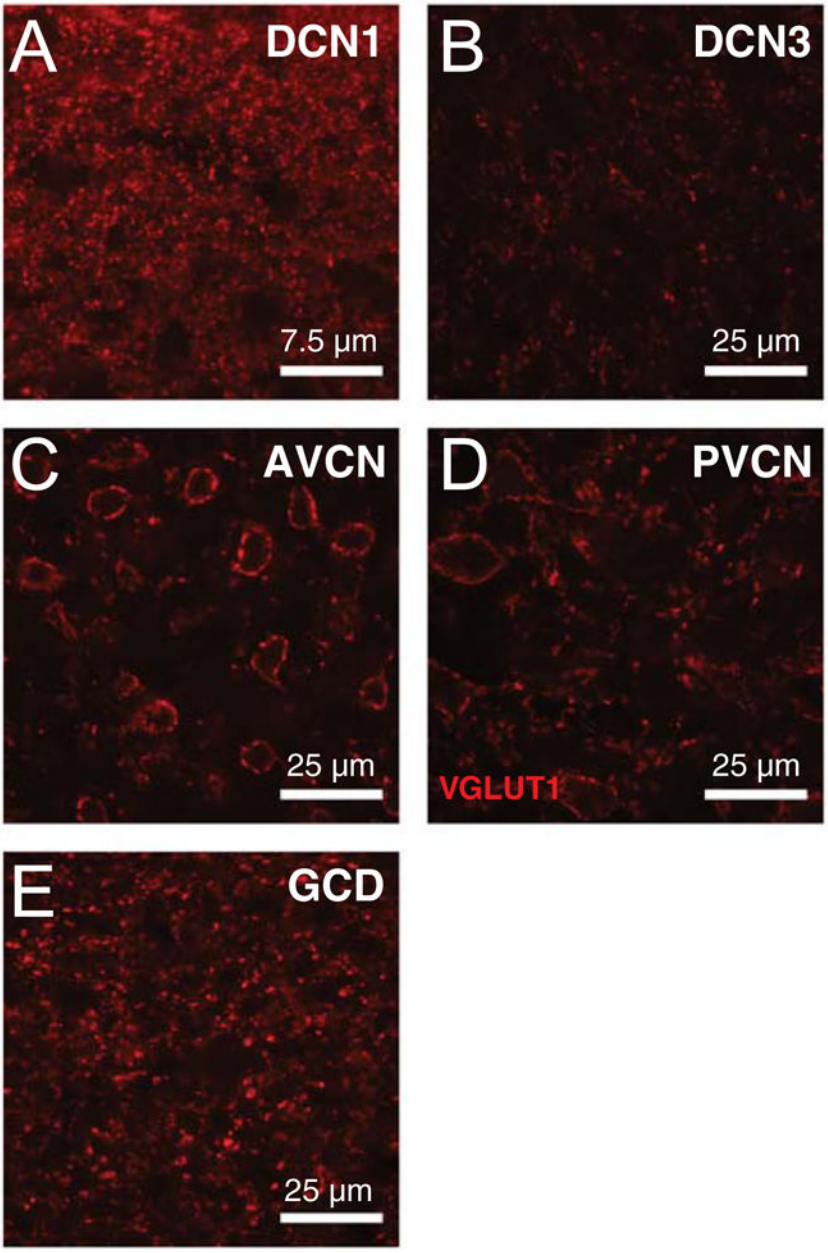

Figure 6: VGLUT1 immunoreactivity in the different regions of the CN.

Immunoreactivity of VGLUT1 in the DCN1 (A), DCN3 (B), PVCN (C), AVCN (D), and GCD (E) of a control animal. The scale bar in panel A represents 7.5 µm; the scale bars in panels B-E represent 25 µm.

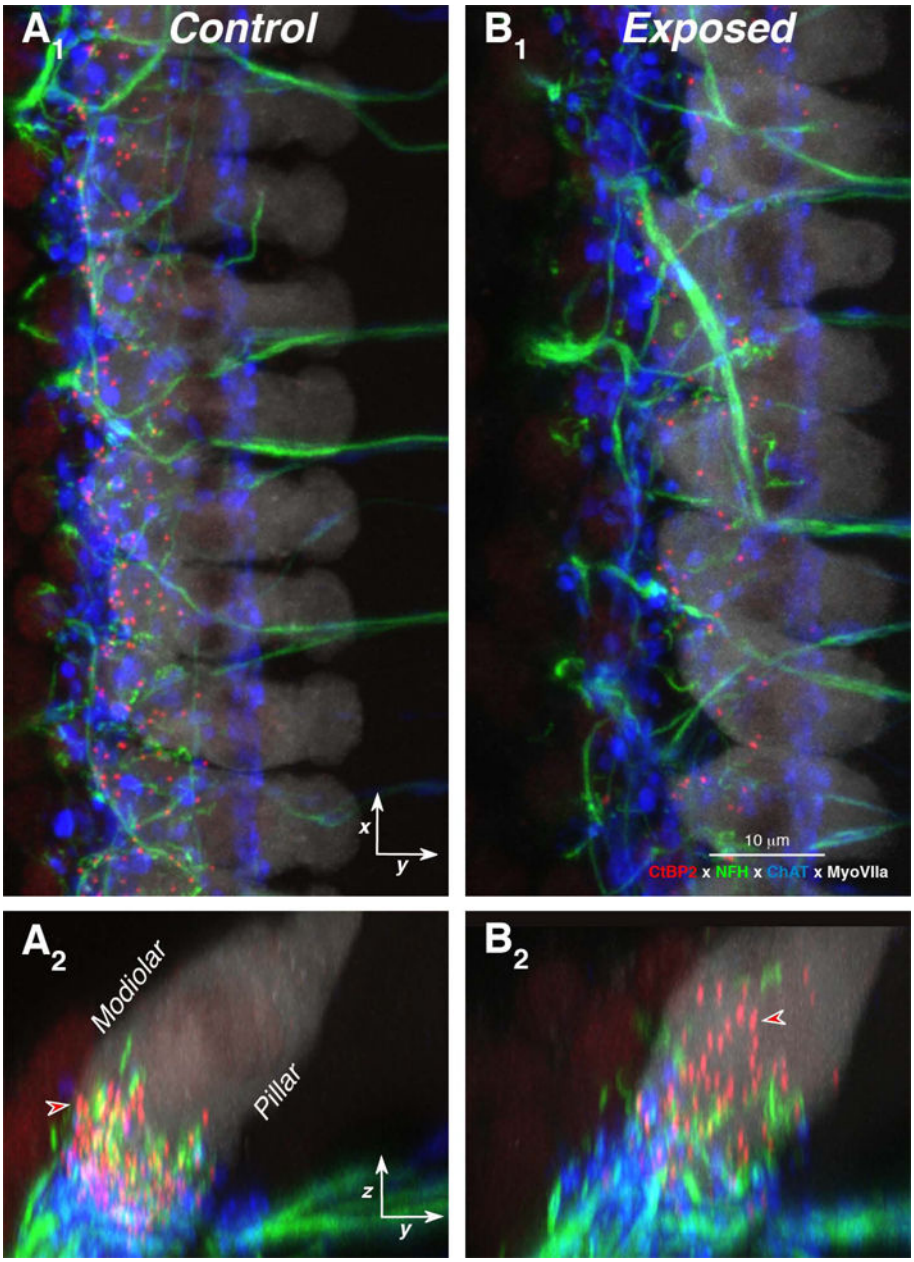

Figure 7: VGLUT1 puncta density was altered in tinnitus animals.

VGLUT1 puncta density in the DCN1 (A), DCN3 (B), PVCN (C), AVCN (D), and GCD (E) for the sham exposed (N; in black), exposed-no-tinnitus (ENT; in blue), exposed-tinnitus (ET; in red), and exposed-tinnitus-treated (ET_T; in green) animals. The vertical axis represents VGLUT1 puncta density (number of puncta/mm^2). Solid bars represent ipsilateral VGLUT1 puncta density, shaded bars represent contralateral VGLUT1 puncta density. * indicates significant differences after post-hoc Tukey-Kramer's test ($p<0.05$) when the 2-way ANOVA was significant for group and side.

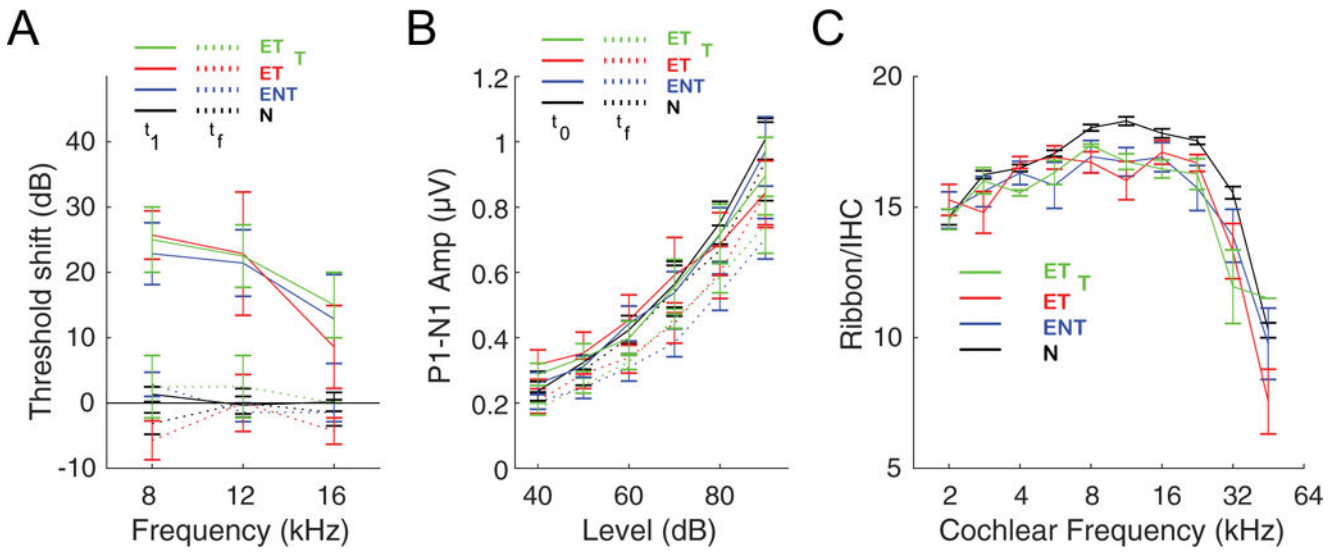

Figure 8: Interaural asymmetry of VGLUT1 immunoreactivity in the AVCN of a tinnitus animal.

VGLUT1 immunoreactivity in the ipsilateral (A, C, E) and contralateral (B, D, F) AVCN of an exposed tinnitus (A, B), an exposed no-tinnitus (C, D), and an exposed tinnitus treated (E, F) animal. Scale bar represents 25 μm.

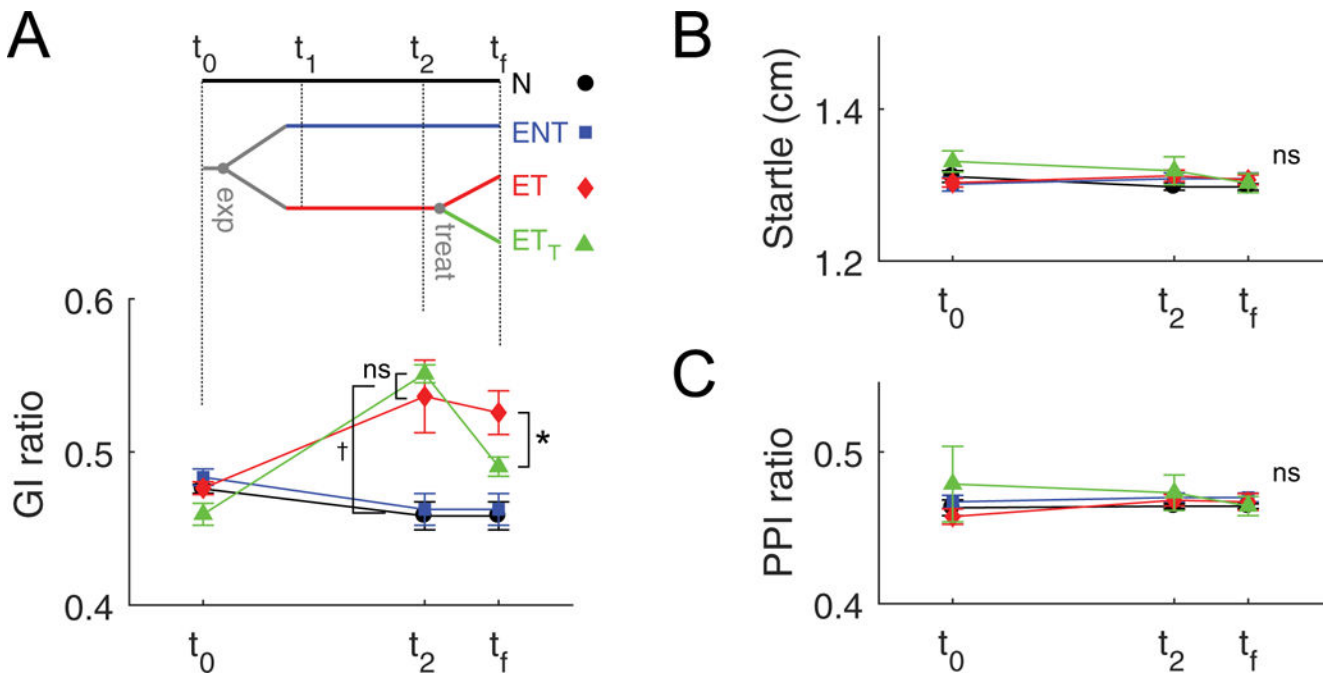

Figure 9: VGLUT2 immunoreactivity in different regions of a control CN.

The scale bar in panel A represents 7.5 μm; the scale bars in panels B-E represent 25 μm.

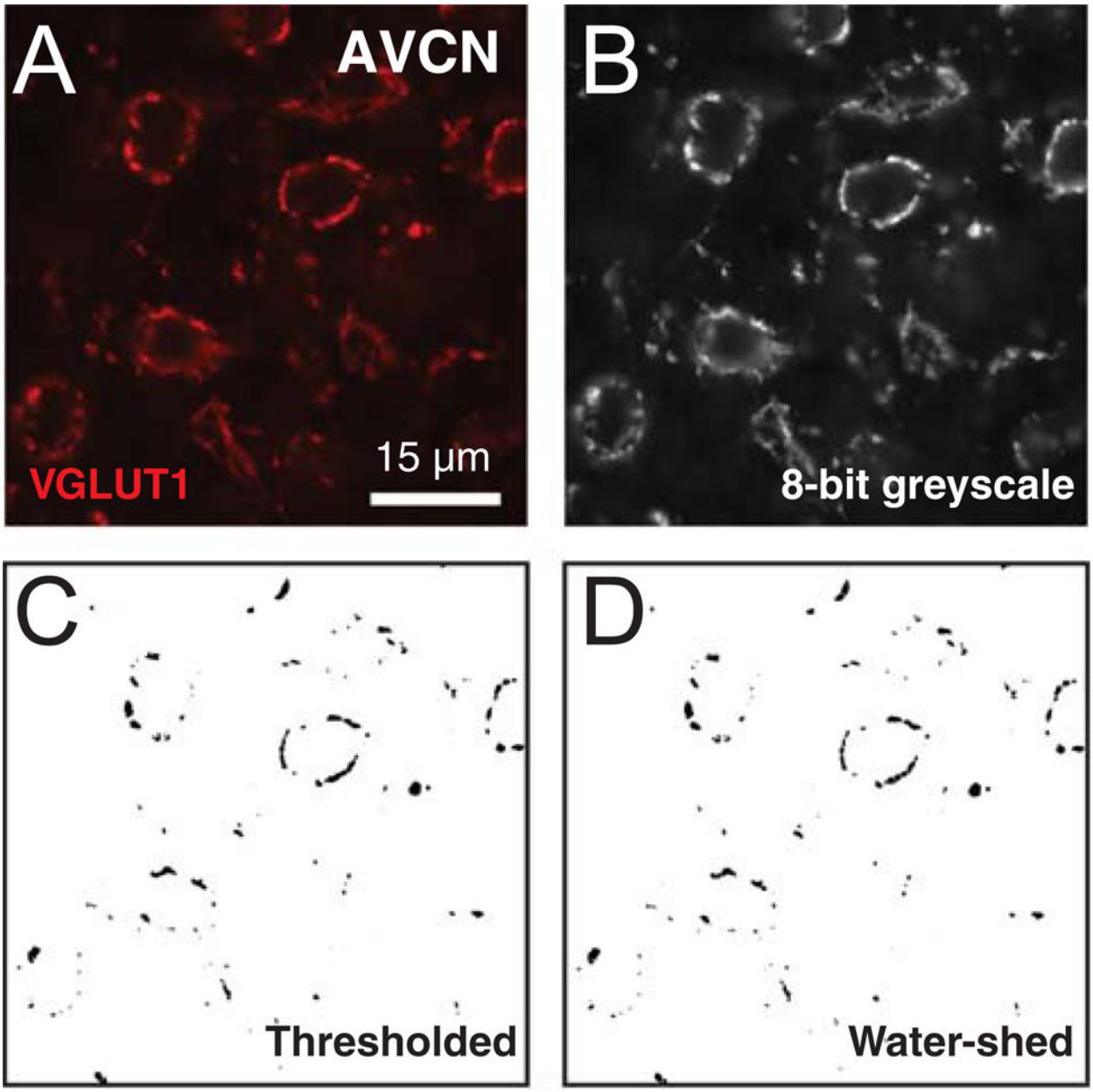

Figure 10: VGLUT2 puncta density was altered in tinnitus animals.

VGLUT2 puncta density (number of puncta/mm^2) in the DCN1 (A), DCN3 (B), PVCN (C), AVCN (D), and GCD (E) for the sham exposed (black), exposed-no-tinnitus (blue), exposed-tinnitus (red), and exposed-tinnitus-treated (green) animals on the ipsilateral (solid bars), and contralateral side (shaded bars). * represents significant differences after post-hoc Tukey-Kramer's test ($p<0.05$).

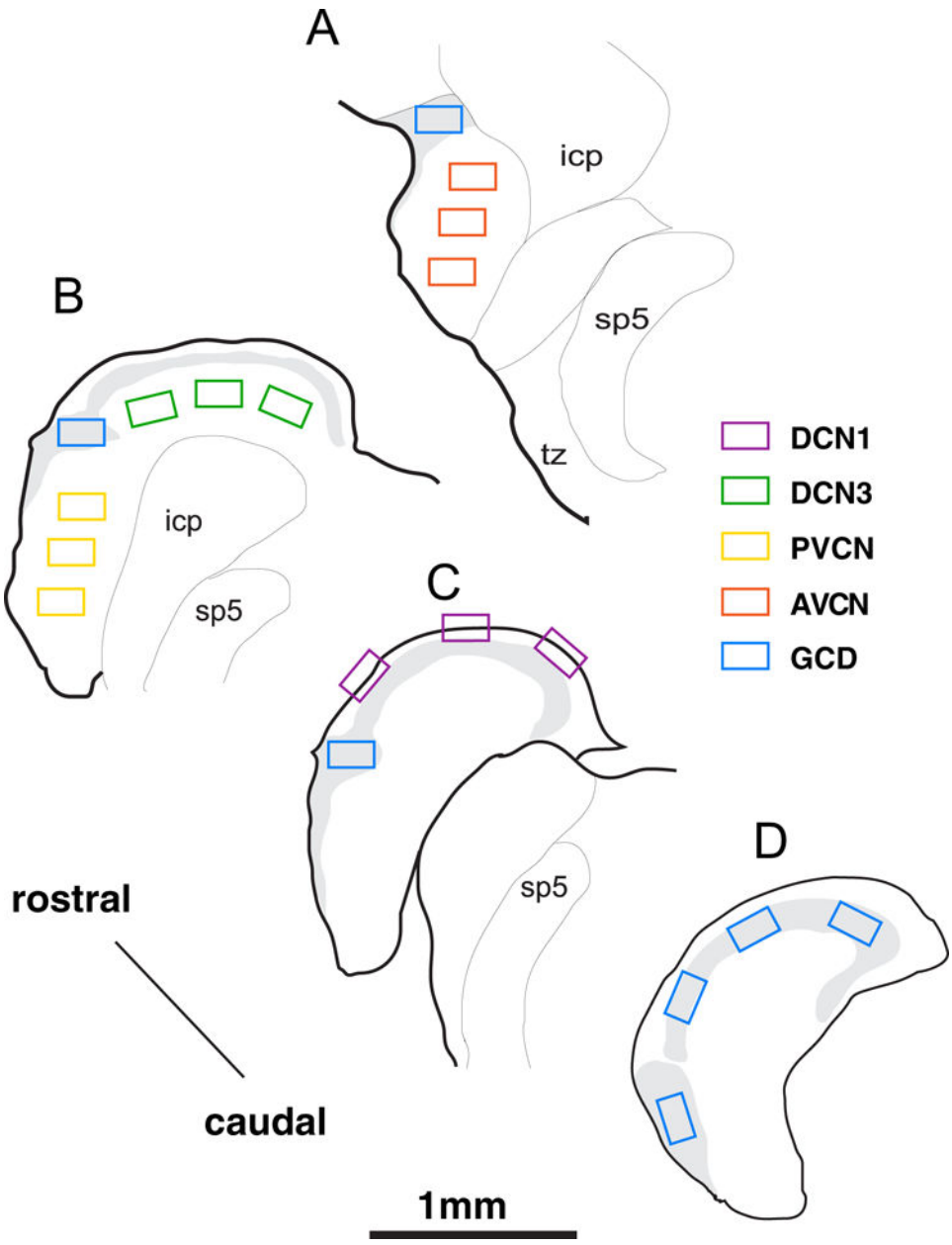

Figure 11: Interaural asymmetry of VGLUT2 immunoreactivity in the AVCN of a tinnitus animal.

VGLUT2 immunoreactivity in the ipsilateral (A, C, E) and contralateral (B, D, F) AVCN of an exposed tinnitus (A, B), an exposed no-tinnitus (C, D), and an exposed tinnitus treated (E, F) animal. Scale bar represents 25 μm.